

*Research article***Self-healing properties of augmented injectable hydrogels over time**Connor Castro¹, Zachary R. Brown² and Erik Brewer^{1,2,*}¹ Dept. of Biomedical Engineering, Rowan University; Glassboro, NJ, USA² ReGelTec, Inc.; Baltimore, Maryland, USA* **Correspondence:** Email: brewere@rowan.edu.

Abstract: Injectable polymers offer great benefits compared to other types of implants; however, they tend to suffer from increased mechanical wear and may need a replacement implant to restore these mechanical properties. The purpose of this experiment is to investigate an injectable hydrogel's self-healing ability to augment itself to a previously molded implant. This was accomplished by performing a tensile strength test to examine potential diminishing mechanical properties with increasing time, as well as dye penetration tests to examine the formation of interfacial bonds between healed areas of hydrogels. There were several time points in between injections that were explored, from 0 min between injections all the way up to 48 h in between injections. The tests showed no statistical differences of the increased injection times compared to the single injection for the tensile test. However, our results showed an increase of mechanical breaks at self-healed joints, as well as a linear regression test showed a decrease in dye diffusion rate as time between injections increase. These results show that the hydrogel has strong self-healing abilities, and as time between injections increase, they mechanical properties will slowly decrease. Based on this, the tests can be applied to other injectable implants and a noninvasive solution to a worn-down implant, as well as show scientific backing to a possibly unique and beneficial self-healing property.

Keywords: hydrogel; self-healing; injectable hydrogel; PVA; color analysis; multiple injections; augmented injections

1. Introduction

Injectable polymers, and more specifically injectable hydrogels, are being increasingly researched in the biomedical field. These therapeutics can cover a large portion of different

procedures, from immunotherapy [1], to orthopedics [2,3], ophthalmic applications [4] and even tissue engineering [5,6] Despite there being a lot of research into this new injectable therapeutic, there is only a limited number of FDA-approved products [4]. As of 2020, there have been 28 approved clinical injectable hydrogel products, with an additional 31 of these devices being in clinical trials [7]. These FDA approved products serve as up-to-date technologies to combat the possible downsides that come with surgically implanted therapeutics.

Traditional surgically-implanted biomedical devices have been a reliable solution to many diseases, illnesses, and injuries; however, they do have their disadvantages, such as requiring invasive implantation procedures, longer hospitalization times, prolonged rehabilitations, blood transfusions, and heavier anesthesia use [2,3]. In contrast, injectable polymers have the potential to relieve these disadvantages associated with their surgically implanted counterparts, as they are significantly less invasive. Injectable polymers have been shown to reduce morbidity in tissue engineering applications by being minimally invasive [5]. For bone tissue engineering, injectable hydrogels can promote healing based off their composition, their ability to manipulate and transfer drugs or cells, and they promote cellular responses while they transition from liquid to gel [3]. Another tissue engineering application is for wound healing, where researchers could use the multifunctionality of injectable hydrogels to promote angiogenesis and proliferation of cells [6]. In the immunotherapy field, injectable hydrogels have advantages over their surgical counterparts by reaching anywhere a needle can go, minimizing tissue damage and inflammatory responses, can flow into the desired space, and form an implant, and generally can be implanted with less technical expertise compared to surgeries [8]. However, a common issue with injectable hydrogels is that they typically require compromising mechanical properties to achieve their injectable properties. This is furthermore exacerbated by the mechanical wear and their reduced durability compared to surgically implanted materials [9].

Self-healing hydrogels offer an attractive trait by counteracting the increased wear experienced due to their reduced mechanical properties. These self-healing hydrogels are able to mimic the self-healing properties seen physiologically, they can be more preserved in the body even after being subjected to natural wear and tear, as well as allowing for multiple injections to act as one implant to replenish diminished therapeutic [9]. Self-healing hydrogels are able to repair itself when damaged, which allows the implant to have a longer lifetime in the patient, as well as save the patient money by limiting extractions of worn-out implants [10]. Injectable self-healing hydrogels have been used as an emerging technology in tissue engineering by repairing cranial bone, cartilage tissue, neural systems, and for wound healing applications [9,11,12]. Their main benefit over non-injectable and non-healable materials is their ability to heal irregular tissue damage [13]. For skin wound healing, self-healing injectable hydrogels are being researched due to traditional hydrogels being broken down, which would cause an inflammatory response and hurt wound healing progress [14]. Also, these self-healing injectable hydrogels are a promising research topic for wound dressings for they are able to recover mechanically to the rapid changing needs of wounds, as well as increase the usage time without compromising the anti-inflammatory and angiogenesis abilities of typical wound dressings [12]. Lastly, for drug delivery, self-healing hydrogels have been shown to have increased control over drug release, as well as been shown to better protect the cells and drugs encapsulated inside the hydrogel [15]. While there has been increased research in this topic, there has been a lack of practical use and only been looked at from a mainly research and academic point of view [15].

Hence, in this study, we sought to investigate an injectable poly(vinyl alcohol) (PVA)-based

hydrogel's self-healing ability to augment itself to previously molded samples. We investigated the self-healing kinetics using both mechanical tensile testing, and interface development using dye-diffusion tests and image analysis.

2. Materials and methods

2.1. Materials

PVA with a molecular weight of $145000 \text{ g}\cdot\text{mol}^{-1}$ was obtained from EMD Millipore Corporation (Billerica, MA). PEG with a molecular weight of $1000 \text{ g}\cdot\text{mol}^{-1}$ and poly(vinyl pyrrolidone) (PVP) with a molecular weight of $40000 \text{ g}\cdot\text{mol}^{-1}$ was obtained from Spectrum Chemical (New Brunswick, NJ) and added in small amounts to better stabilize the hydrogel network through interchain hydrogen bonding. Deionized (DI) water was obtained on-site using a Millipore Milli-Q system (Darmstadt, Germany). Barium Sulfate was obtained from Emprove through MilliporeSigma (Burlington, MA) Calcein, research grade, was obtained from MP Biomedicals, LLC (Solon, OH). Methylene Blue solution obtained from Sigma Life Sciences (St. Louis, Missouri).

2.2. Hydrogel preparation

Hydrogels were prepared using an adapted theta solution method previously described by LaMastro [16]. Briefly, aqueous solutions of PVA and PVP were prepared in triplicate by autoclaving the previously mentioned raw materials with DI water at $121 \text{ }^\circ\text{C}$ and 30 psi for 30 min, within 10 min after the first autoclave cycle, the solution was stirred manually by spatula to ensure complete homogenization of the two polymers. Barium sulfate was then added as a radiocontrast agent and mixed into the solution. PEG was added so that the final composition of the hydrogel was approximately 12.4% PVA, 0.1% PVP, 61.7% DI water, 8.3% Barium Sulfate, and 17.5% PEG, and the solution was again homogenized by manual stirring for 3 min. The polymers were allowed to react and form physical crosslinks at room temperature for 3 h. After the reaction was complete, supernatant was carefully removed, and the gel was autoclaved for a second cycle under the same conditions. A second supernatant was removed after a brief period of cooling at room temperature. For the visual studies, approximately 0.1 g of Methylene Blue solution or Calcein were added to the 50 g portions of hydrogel after the final step. The hydrogel was autoclaved after the second supernatant was removed, then the dyes were poured into the gels and stirred.

2.3. Injection mold process

3D printed ring molds were created with there being full ring molds and semi-circular ring molds to make half samples. Full ring molds created a continuous ring of hydrogel and were considered to be baseline samples. The half molds were made to represent worn implants, which would then be subject to a second injection after a certain period to create a continuous ring from two separate injections, with each half injection having a volume of (625 mm^3) . The cross-sectional dimensions of the ring mold are a $5 \text{ mm} \times 5 \text{ mm}$ square, and the outer diameter of the mold is 25 mm, leading to a total volume of approximately 1250 mm^3 of hydrogel for a full mold. Baseline samples were fully injected into the full molds, then any excess hydrogel was removed from the mold and

discarded. 15 min samples were prepared by putting a silicone mold, having the same volume as the half mold (625 mm^3) into the full mold to turn the previous full mold into a half mold, having the same volume as the previously described half mold, and inject hydrogel into the remaining half of the full mold and after 15 min the mold was removed, creating a 625 mm^3 half mold. Then the second injection was done. The silicone mold was only used for this time point because the hydrogel was too soft to be taken out of one mold and put into another while maintaining its shape, so this allowed the hydrogel to sit in one full mold while still being able to give the same two semi-circular injections. For the rest of the time points, the first injection would take place in the 3D printed semi-circular mold, then moved into a full mold for a second injection. Since in this injected state the hydrogel is liquid, they can be stamped into the mold to ensure that they take the shape of the mold and remove any air pockets. Once each injection was complete, the sample inside its mold would be wrapped in Parafilm and stored in a 6-well well plate that contained water, which was not in contact with the samples, to keep the samples hydrated.

2.4. Mechanical testing

The testing was done in a $37 \text{ }^\circ\text{C}$ warm room using a Shimazu EZ-SX mechanical tester with a 500N load cell. The samples would be taken out of the molds and their joints would be marked, if applicable, as seen in Figure 1. The sample was rigged onto two shackle-like attachments that would loop into the open circle of the ring mold. Then the sample would be pre-tested to 2 N and then pulled at 200% strain/minute to failure. Once the sample broke, the max force, moduli for 5–10 N and 10–15 N were calculated.

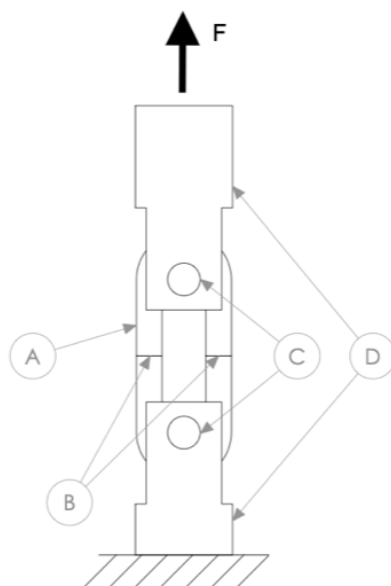


Figure 1. A diagram showing the tensile testing set up of a two-injection ring sample is shown above. (A) Test sample/ring mold, (B) is the marked augmentation sites or self-healed sites, (C) are shackle pins that keep the sample attached to the mechanical tester, and (D) are the testing fixtures. The arrow above the testing fixture shows the direction of force applied by the mechanical tester.

2.5. Visual studies

First, the hydrogel was prepared as normal, but before they were used for testing, the hydrogel was mixed with either Methylene Blue solution or Calcein, Research Grade. Once they were dyed, they were used for this study. The injections were done in a 12-well well plate that contained water in separate wells from the hydrogel to keep the samples hydrated. For the test, a yellow injection was done in one plate, and a blue injection was done in a separate plate. Inside the injected plates were two silicone molds that were made to cover half of the well, leaving two half-moon like pieces of hydrogel. After a period of time, a second injection was done to the two older injections of the opposite color (e.g., the first yellow injection would be paired with a fresh blue injection) and put together in a new clean well, so there would be two adjacent wells containing two blue/yellow, blue/yellow full wells, forming two samples to be tested at a time. To ensure there was no excess dye, before any samples contacted each other, they were patted with a dry paper towel, then immediately after were assembled to form the samples described previously.

While the samples sit, the well plate was covered, as well as some empty wells contained water to prevent hydrogel drying. The well plate was set onto a ring stand and a phone with a time lapse app was placed below it. A lamp was lighting the sample from below to allow for consistent lighting throughout the time lapse. The time lapse would immediately take a picture, and then would take a picture once every hour for 48 h. Once 48 h have passed, the time lapse was obtained and cut up so each sample would have pictures that were created at every 5 h starting at 1 h after the second injection. These pictures were then having their backgrounds colored in both blue and yellow. These pictures were then run through an ImageJ macro program multiple times to obtain the total sample area with the blue and yellow background, the blue area of the sample, and the yellow area of the sample.

Analysis studies were done using ImageJ (Bethesda, Maryland) and the macro used was created by Strock [17]. This was done through manually thresholding the colors for each sample and was using the same threshold for each picture in the sample. To set the threshold, the initial image was put into a color thresholding slider, where the program allows the user to control the RGB values that the user would want to threshold. This threshold creates a new image which only has the color and part of the sample that is desired. These slider options are then applied to each image of the sample. To ensure that blue and yellow are successfully being threshold, the sliders were set to the initial image and compared to the last image, where there should be no green included in either of the thresholds. The reason the area of a blue background set of images and yellow set of images is due to the images not being the exact same sizes, which allows for the areas of blue and yellow be standardized and remove the effect of image size variation from the data analysis. Also, to properly threshold the sample, the yellow background would be applied on the images where the blue was threshold, so the background and yellow part of the sample can be removed in a single thresholding process, and vice versa with the blue background and yellow sample.

To standardize the test and account for error, every initial image would have assumed 0% green area, and if this value was not zero, the non-zero initial value would be subtracted from the rest of the time lapsed images, for example, if the initial image for the 1st 1 h samples was 3% green, then that 3% would be subtracted from the 5 h, 10 h, etc. percentages. To further standardize the samples, the percentage of blue/yellow at a particular time point would be divided by the initial percentage of blue/yellow to remove any error from blue or yellow gel area variation from the data collection.

These ratios would be subtracted from 2, since the blue and yellow initial areas after the standardization would be 100% each, then this value would be divided by two to get the percent of green in the sample. This was done for each image in a sample, and the thresholds would change between samples based off blue and yellow saturation in the hydrogels, but they would be kept the same within the sample to get accurate changes in green throughout the timelapse.

2.6. Statistical analysis

The linear regression tests and the multiple comparison ANOVA analysis tests were all performed in GraphPad Prism 9 (San Diego, California).

3. Results

3.1. Mechanical testing

To assess the strength of the hydrogels self-healing properties with previously injected hydrogel pieces over time, a mechanical tensile strength test was performed to obtain the hydrogels breaking strength. An example of the data received during the tensile test can be seen in Figure 2. The resultant averages and standard deviations of the tensile tests based on time in between injections can be seen in Figure 3. The time point with the highest average breaking force was the full, single injected ring mold, with an average breaking force of 36.26 ± 16.71 N, and the lowest being the 24 h in between injections, with an average breaking force of 25.73 ± 8.27 N. However, an ANOVA multiple comparison test showed no significant difference between any of the time points.

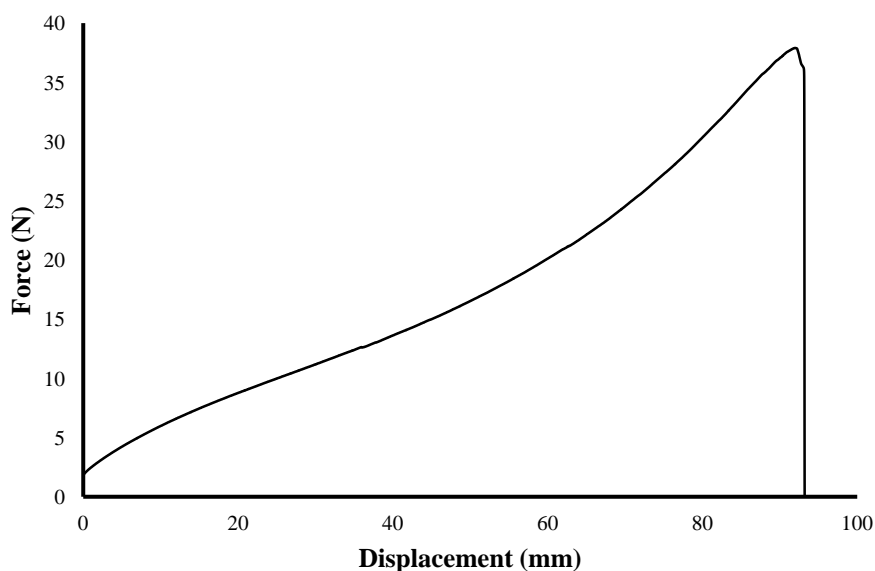


Figure 2. Tensile testing of healed PVA hydrogels.

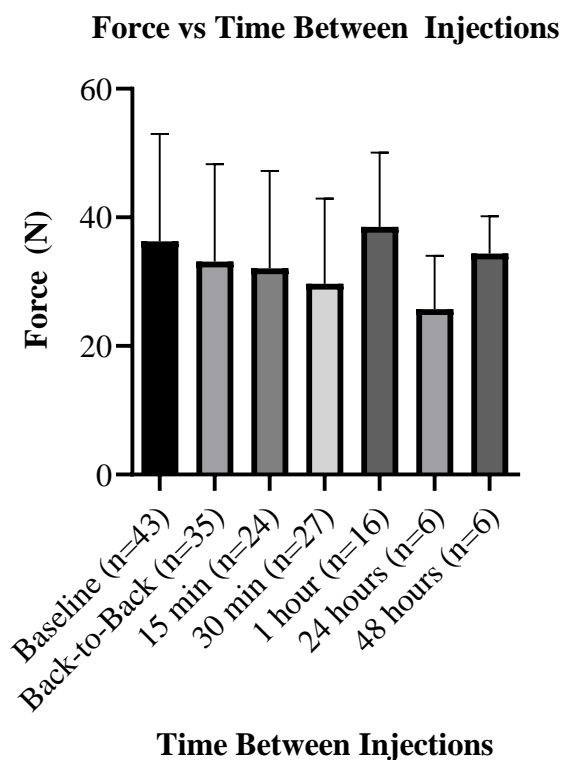


Figure 3. Breaking force of self-healed hydrogels. Baseline samples represent control samples made from a single continuous injection, while all other samples comprise of samples made of two injections with variable time in between injections. Data is presented in a mean \pm SD format.

The locations upon where the hydrogel broke was recorded in Table 1. The lowest percentage of samples that broke at the self-healed site was the 0min injection samples, with a percentage of 24%. This percentage increased as time between injections increased, with the highest percentage of breakage at the self-healed site occurring at 48 h, with a percentage of 67%.

Table 1. Hydrogel breaking point location.


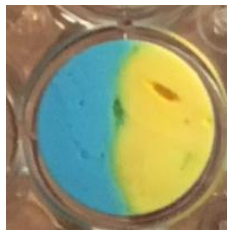

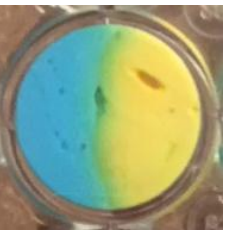
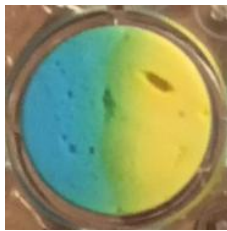

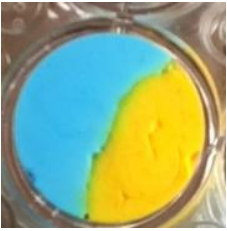

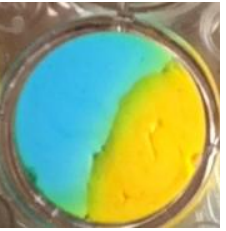
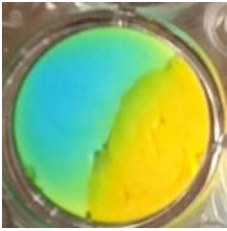
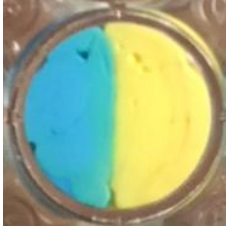

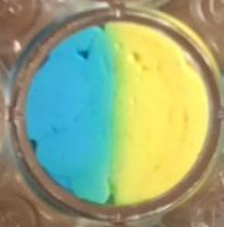

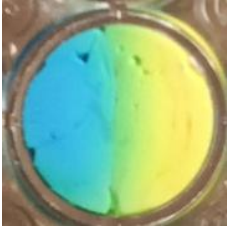

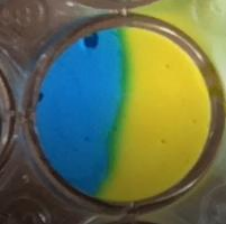
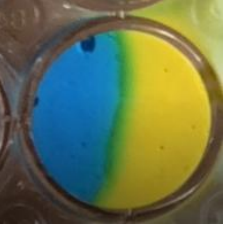
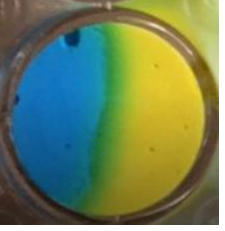
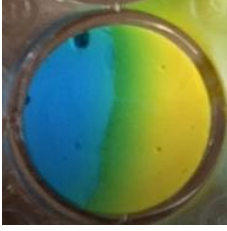
Sample	Samples that broke at joint	Total samples tested	% Samples that broke at joint
Simultaneous	-	43	-
0 min	8	34	24%
15 min	10	24	42%
30 min	11	27	41%
1 h	10	16	63%
24 h	3	6	50%
48 h	4	6	67%

3.2. Visual analysis

Table 2 shows examples of the samples tested and how the amount of green area can change

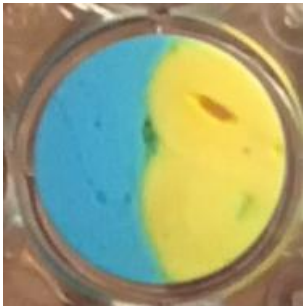
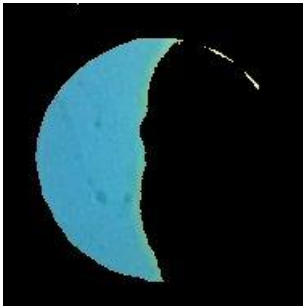
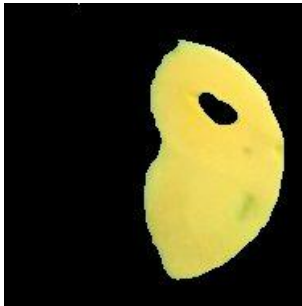
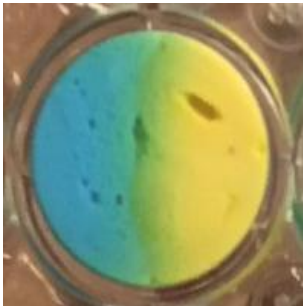
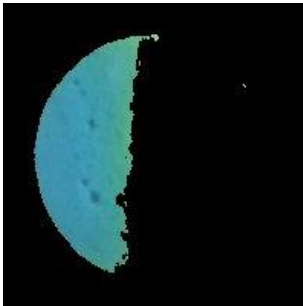

with respect to time. The y-axis in the table shows the time between the first injection and the second injection, and the x-axis is the amount of time that sample had to set. The amount of time the hydrogel had to set had its green area calculated after every 5 h, as well as at 48 h, and the max time that was analyzed for the set hydrogel was at 48 h. Table 3 shows an example of how the area of green was determined. The 0 h time point shows the initial threshold of the blue and yellow areas of the hydrogel samples, as well as the original image it was taken from. The 48 h time point shows how the thresholding program is able to eliminate the green area growth from the sample. Also, it shows the percent of blue and yellow initially compared to their percentages after 48 h.

Table 2. Visual progression of dye diffusion through healed interface.

	0 h	5 h	10 h	20 h	48 h
0 h					
1 h					
24 h					
48 h					

Rows represent samples with differing amounts of times between injections of separately-dyed hydrogel, while columns show the time-laps of each of those gels over 48 h.

Table 3. Quantitative analysis of dye penetration.

Time	Original image	“Blue” analysis	“Yellow” analysis
0 h			
	100%	42%	52%
48 h			
	100%	36%	43%

A linear regression test was performed on the slopes of the average percentage of green as time between injections increased, with respect to time (Figure 4) and the results can be seen in Table 4. There was no significant difference between the 24 h and 48 h groups, as well as the 0 h and 1 h groups. The 0 h and 1 hour groups were statistically different from the 24 h group and the 48 h group.

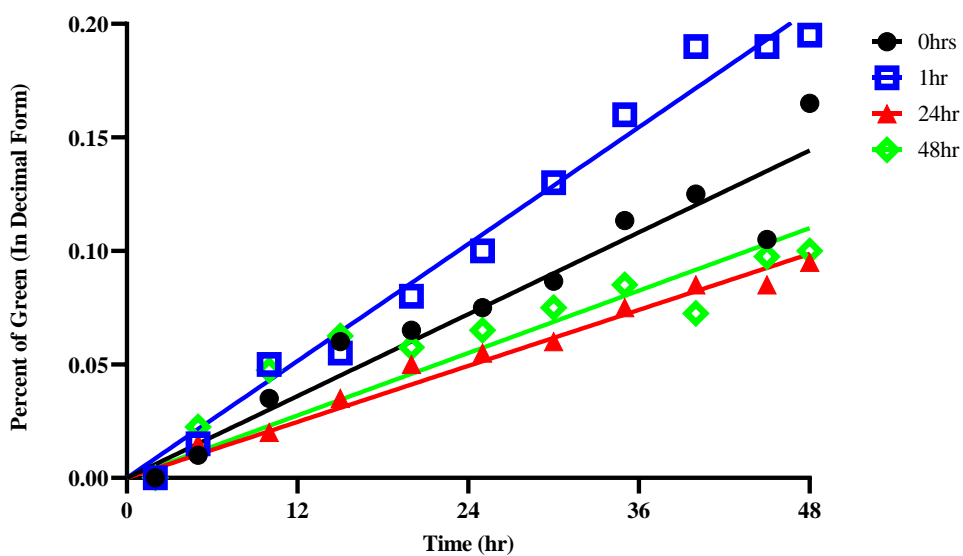
Linear Regression of Green Percentages of Different Second Injection Times versus Setting Time**Figure 4.** Scatter plot of dye diffusion with linear regression lines.

Table 4. Best fit line statistics.

Time between injections	Best-fit slopes	Standard error slopes	Confidence intervals (95%)
0 h	0.003004	0.0001729	0.002658 to 0.003350
1 h	0.004291	0.0005392	0.003166 to 0.005415
24 h	0.002055	0.0001683	0.001704 to 0.002406
48 h	0.002291	0.0001697	0.001949 to 0.002633

4. Discussion

To assess PVA hydrogels self-healing ability to augment to older injected samples, mechanical tensile strength tests were performed to obtain the hydrogel's breaking strength. For these tests, there was a downwards trend in the breaking forces of the samples as time increased between injections, however there was no significant difference observed (Figure 3). To further analyze the mechanical impact of increasing time between molds, break location was also observed, and there was also an increase in the percentage of samples that would break at the interface between the two injections as time between injections increased (Table 1). The increase in breaking at the self-healed site combined with the lower breaking forces at increased times showed that there was a weaker interface and strength at self-healed interfaces when the time increased between injections.

To support this hypothesis, dye diffusion tests were performed to visually assess this diffusion rate. For the visual test, several papers have used dyed samples to visually demonstrate successful self-healing, where the diffusion of dyes from different samples in contact would producing a new color combined color, was used to indicate successful interface formation and thus showing successful self-healing ability [10,12,18,19]. These methods were implemented here as well, with the added quantification of the dye mixing for improved evaluation, and used the dye diffusion as a metric for measuring self-healing, for dye permeability and interface has been shown to be influenced by self-healing [20].

Using a linear regression test, there was no significant difference of the 24 h group and the 48 h group, as well as no significant difference between the 0 h and 1 h group. However, there was a significant difference between the 0 h/1 h groups and the 24 h/48 h groups (Table 4). This demonstrates that there is a difference in the diffusion rate of the samples depending on the time between injections. This also supports why there is an increase in breaking points at the joining sites on the later time points, for there is a weaker interaction between the two injections. This weaker interaction is also seen in the tensile strength test, for there is a downward trend in the breaking forces of the increased time between injections. These three tests show a decrease in mechanical properties of the self-healed hydrogel compared to a single piece of hydrogel.

The reason for this weaker interface and mechanical properties likely is caused by the bond orientation as the hydrogel becomes more solid, where it would look to become more stable structurally. When the time between injections decrease, there is less time for the bonds of the initial implant to become structurally stable, allowing those bonds to happen more frequently with the second injection, which is a liquid and can bond more readily to the older implant. The more bonds that can form at the interface of the two injections, the greater the interface strength and mechanical strength of the full augmented implant.

The results of this experiment could provide some deeper insight and practical use for other injectable implants. Hydrogel implants have been shown to be able to be worn down overtime, and

thus there is a need to investigate ways of repairing or augmenting these implants using non-invasive means [9]. These studies, using PVA-based hydrogels as a representative injectable formulation, showed that additional injections could be performed to augment previously implanted materials with minimal decrease of the mechanical strength of the implant.

5. Conclusions

The purpose of these studies was to examine the ability of injectable hydrogels to self-heal by augmenting a new injection with a previous implant and look at how the combined implant's mechanical properties would change as a function of time. The results from these studies demonstrated that the hydrogel tested had a strong ability to self-heal with augmented material with minimal decrease in mechanical performance. Future implications of this test could expand to other hydrogels or injectable implants that are worn down, for this could allow for investigation of implants that can receive augmentation injections or implants with having minimal mechanical degradation in a minimally invasive manner.

Acknowledgements

The authors wish to thank educational materials provided by Christopher Strock on the open-source ImageJ macro created for color analysis.

Conflict of interest

Funding for this project was provided by ReGelTec, Inc., which is investigating injectable polymers for commercial applications.

References

1. Leach DG, Young S, Hartgerink JD (2019) Advances in immunotherapy delivery from implantable and injectable biomaterials. *Acta Biomater* 88: 15–31. <https://doi.org/10.1016/j.actbio.2019.02.016>
2. Raucci MG, D'Amora U, Ronca A, et al. (2020) Injectable functional biomaterials for minimally invasive surgery. *Adv Healthc Mater* 9: 1–20. <https://doi.org/10.1002/adhm.202000349>
3. Kondiah PJ, Choonara YE, Kondiah PP, et al. (2016) A review of injectable polymeric hydrogel systems for application in bone tissue engineering. *Molecules* 21: 1580. <https://doi.org/10.3390/molecules21111580>
4. Wang K, Han Z (2017) Injectable hydrogels for ophthalmic applications. *J Control Release* 268: 212–224. <https://doi.org/10.1016/j.jconrel.2017.10.031>
5. Kretlow JD, Young S, Klouda L, et al. (2009) Injectable biomaterials for regenerating complex craniofacial tissues. *Adv Mater* 21: 3368–3393. <https://doi.org/10.1002/adma.200802009>
6. Cui L, Li J, Guan S, et al. (2021) Injectable multifunctional CMC/HA-DA hydrogel for repairing skin injury. *Mater Today Bio* 14: 100257. <https://doi.org/10.1016/j.mtbio.2022.100257>
7. Mandal A, Clegg JR, Anselmo AC, et al. (2020) Hydrogels in the clinic. *Bioeng Transl Med* 5: 1–12. <https://doi.org/10.1002/btm2.10158>

8. Leach DG, Young S, Hartgerink JD (2019) Advances in immunotherapy delivery from implantable and injectable biomaterials. *Acta Biomater* 88: 15–31. <https://doi.org/10.1016/j.actbio.2019.02.016>
9. Li Q, Liu C, Wen J, et al. (2017) The design, mechanism and biomedical application of self-healing hydrogels. *Chinese Chem Lett* 28: 1857–1874. <https://doi.org/10.1016/j.ccllet.2017.05.007>
10. Kang M, Liu S, Oderinde O, et al. (2018) Template method for dual network self-healing hydrogel with conductive property. *Mater Design* 148: 96–103. <https://doi.org/10.1016/j.matdes.2018.03.047>
11. Lü S, Bai X, Liu H, et al. (2017) An injectable and self-healing hydrogel with covalent cross-linking: In vivo for cranial bone repair. *J Mater Chem B* 5: 3739–3748. <https://doi.org/10.1039/C7TB00776K>
12. Liang J, Zhang K, Li J, et al. (2022) Injectable protocatechuic acid based composite hydrogel with hemostatic and antioxidant properties for skin regeneration. *Mater Design* 222: 111109. <https://doi.org/10.1016/j.matdes.2022.111109>
13. Xu Y, Li Y, Chen Q, et al. (2018) Injectable and self-healing chitosan hydrogel based on imine bonds: Design and therapeutic applications. *Int J Mol Sci* 19: 2198. <https://doi.org/10.3390/ijms19082198>
14. Yu H, Liu Y, Yang H, et al. (2016) An injectable self-healing hydrogel based on chain-extended PEO-PPO-PEO multiblock copolymer. *Macromol Rapid Commun* 37: 1723–1728. <https://doi.org/10.1002/marc.201600323>
15. Tu Y, Chen N, Li C, et al. (2019) Advances in injectable self-healing biomedical hydrogels. *Acta Biomater* 90: 1–20. <https://doi.org/10.1016/j.actbio.2019.03.057>
16. LaMastro V, Brewer E, Lowman AM (2020) Crystallinity, reversibility, and injectability of physically crosslinked poly(vinyl alcohol) and poly(ethylene glycol) hydrogels. *J Appl Polym Sci* 137: 48706. <https://doi.org/10.1002/app.48706>
17. Strock C (2021) Protocol for extracting basic color metrics from Images in ImageJ/Fiji. Available from: <https://zenodo.org/record/5595203#.Y1DSZHbMK3D>.
18. Li G, Wu J, Wang B, et al. (2015) Self-healing supramolecular self-assembled hydrogels based on poly(L-glutamic acid). *Biomacromolecules* 16: 3508–3518. <https://doi.org/10.1021/acs.biomac.5b01287>
19. Luo F, Sun TL, Nakajima T, et al. (2015) Oppositely charged polyelectrolytes form tough, self-healing, and rebuildable hydrogels. *Adv Mater* 27: 2722–2727. <https://doi.org/10.1002/adma.201500140>
20. He X, Zhang C, Wang M, et al. (2017) An electrically and mechanically autonomic self-healing hybrid hydrogel with tough and thermoplastic properties. *ACS Appl Mater Interfaces* 9: 11134–11143. <https://doi.org/10.1021/acsami.7b00358>



AIMS Press

© 2023 the Author(s), licensee AIMS Press. This is an open access article distributed under the terms of the Creative Commons Attribution License (<http://creativecommons.org/licenses/by/4.0>)